

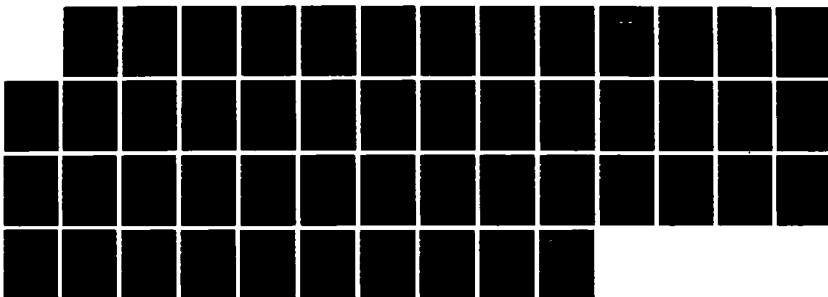
AD-A190 575

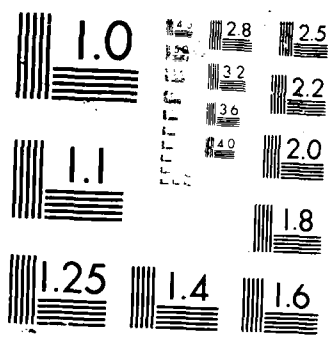
MODELING THE EFFECTS OF HEAVY CHARGED PARTICLES ON
MOSFETS (METAL-OXIDE-S... (U) AIR FORCE INST OF TECH
WRIGHT-PATTERSON AFB OH SCHOOL OF ENGI... K H KATTNER
MAR 88 AFIT/GEP/GNE/88H-4 F/G 9/1

1/1

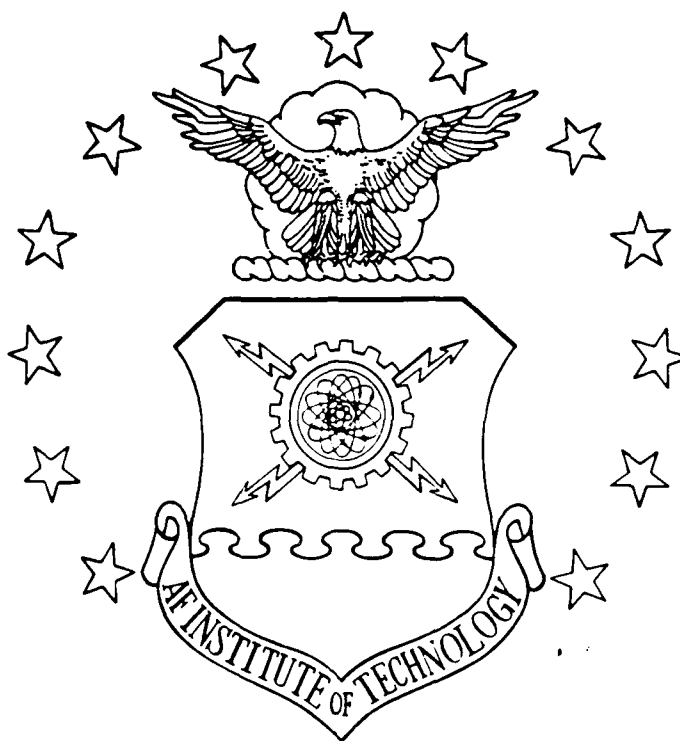
UNCLASSIFIED

NL





AD-A190 575



MODELING THE EFFECTS OF HEAVY
CHARGED PARTICLES ON MOSFETS

THESIS

Kevin M. Kattner
Captain, USAF

AFIT/GEP/GNE/88M-4

DTIC
ELECTE
APR 1988
S E D

DEPARTMENT OF THE AIR FORCE
AIR UNIVERSITY

AIR FORCE INSTITUTE OF TECHNOLOGY

Wright-Patterson Air Force Base, Ohio

This document has been approved
for public release and sale in
distribution is unlimited.

88 3 30 039

AFIT/GEP/GNE/88M-4

MODELING THE EFFECTS OF HEAVY
CHARGED PARTICLES ON MOSFETS
THESIS

Kevin M. Kattner
Captain, USAF

AFIT/GEP/GNE/88M-4

Approved for public release; distribution unlimited

DTIC

901

AFIT/GEP/GNE/88M-4

MODELING THE EFFECTS OF
HEAVY CHARGED PARTICLES ON
METAL-OXIDE-SEMICONDUCTOR
FIELD EFFECT TRANSISTORS

THESIS

Presented to the Faculty of the School of Engineering
of the Air Force Institute of Technology
Air University
In Partial Fulfillment of the
Requirements for the Degree of
Master of Science in Nuclear Engineering

Kevin M. Kattner, B.S.
Captain, USAF

March 1988

Accession For	
DTIC GRA&I	<input checked="checked" type="checkbox"/>
DTIC TAB	<input type="checkbox"/>
Unannounced	<input type="checkbox"/>
Justification	
By	
Distribution/	
Availability Codes	
Dist	Avail and/or Special
A-1	

Approved for public release; distribution unlimited

Preface

The purpose of this study was to model the effect charged particle radiation has on the working parameters of metal-oxide-semiconductor field-effect transistors (MOSFETs). There are two individuals I would especially like to thank. One is my thesis advisor Michael Sabochick, for the helpful advice and guidance he provided throughout the project. The other is Roger Tallon of the Air Force Weapons Laboratory, who originally suggested this as a possible thesis topic, and provided an (at the time) unpublished copy of their experimental results.

Table of Contents

Preface	ii
List of Figures	iv
Abstract	v
I. Introduction and Background	1
II. Theory	9
Columnar Phenomena	9
Bulk Phenomena	15
Interface Phenomena	15
Threshold Voltage vs Dose	17
III. Results and Analysis	22
IV. Conclusion	28
Appendix	29
Bibliography	38
Vita	40

List of Figures

1.	Schematic of an N-Channel MOSFET	2
2.	Sequence of Events Associated with Irradiation of MOSFET	3
3.	P-Channel MOSFET Damage Sensitivity as a Function of Particle Energy and Angle of Incidence	4
4.	N-channel MOSFET Damage Sensitivity as a Function of Particle Energy and Angle of Incidence	5
5.	Change in Threshold Voltage as a Function of Dose and Angle of Incidence for Applied Gate Voltage of -5 Volts	6
6.	Change in Threshold Voltage as a Function of Dose for 80 Degree Angle of Incidence and Gate Voltages of -5 and -10 Volts	7
7.	Change in Threshold Voltage as a Function of Dose for 45 Degree Angle of Incidence and Gate Voltages of -2 and -5 Volts	8
8.	Charged Particle Track Through the Oxide	11
9.	Electron and Hole Columns Moving Under the Influence of Arbitrary Electric Field	13
10.	Schematic Cross Section of MOSFET with Arbitrary Areal Charge Density	19
11.	Schematic Cross Section of MOSFET with Arbitrary Charge Density	20
12.	Fraction Yield as a Function of Particle Energy and Angle of Incidence	23
13.	Fraction Yield as a Function of Electric Field and Angle of Incidence	24
14.	Threshold Voltage Change As a Function of Dose, Angle of Incidence, and Trapping Fraction	25
15.	Electric Field Within the Oxide from an Evenly Distributed Charge Density	27

Abstract

A simple model to characterize the effects of heavy charged particles on metal-oxide semiconductor field-effect transistors (MOSFET) is presented. The model is applied to experimental results provided by the Air Force Weapons Laboratory, and an attempt made to simulate saturation phenomena observed in the threshold voltage change. The model assumes all trapped holes are within a few nanometers of the oxide-semiconductor interface, and takes into account the resultant counter electric field, and its effect on the yield fraction escaping recombination. An equation relating threshold voltage change as a function of dose is derived and used, but does not duplicate the saturation effect. This is because charge trapped near the interface reduces the internal oxide electric field very little. However, similarities in p-channel and n-channel MOSFET damage sensitivities indicate considerable bulk charge trapping. This would modulate the internal electric field considerably. To determine whether this accounts for saturation will necessitate refinement of the model, taking hole transport and bulk trapping into account.

MODELING THE EFFECTS OF HEAVY CHARGED PARTICLES ON METAL-OXIDE- SEMICONDUCTOR FIELD EFFECT TRANSISTORS

I. Introduction and Background

One of the most important devices used in very-large-scale integrated circuits is the metal-oxide-semiconductor field-effect transistor (MOSFET). Figure 1 shows a schematic of an n-channel MOSFET. The device works as follows. When a positive voltage is applied to the gate, a strong electric field sets up through the gate oxide and penetrates into the p-type Si substrate. In the region just beneath the gate oxide, this field repels the majority carriers (which, for n-channel MOSFETs, are holes) and attracts minority carriers (electrons), thus forming an inversion layer. With a potential difference applied between source and drain, current flows through this inversion layer and the device is considered "on". The operation of a p-channel MOSFET is similar, only the p-type and n-type materials are reversed, and a negative voltage is applied to the gate contact.

MOSFETs are very sensitive to the effects of ionizing radiation. The sequence of events associated with irradiation of an n-channel MOSFET is shown in Figure 2. Ionizing radiation, such as gamma-rays, electrons, and heavy charged particles, initially create many electron-hole pairs throughout the gate oxide. A certain fraction of these pairs are then annihilated through recombination. The positive applied voltage rapidly sweeps the remaining electrons from the oxide and into the metal gate contact. The holes transport more slowly toward the gate-semiconductor interface, where a certain fraction are caught in deep hole traps

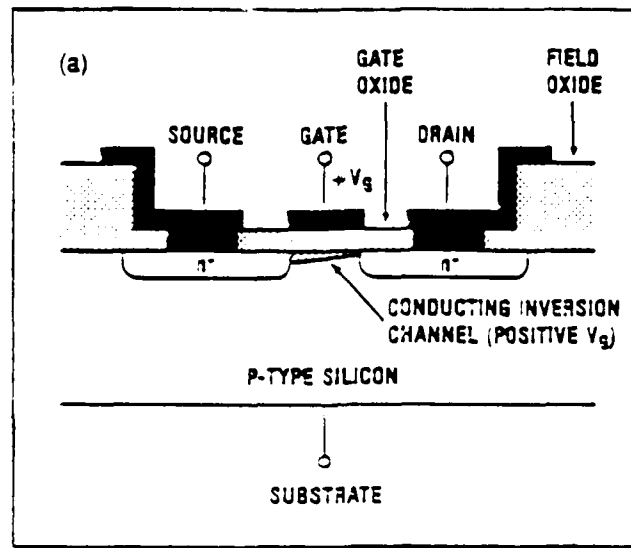


Figure 1. Schematic of an N-channel MOSFET (Ref 1:22)

and the rest disappear into the semiconductor. These trapped holes permanently alter the electric parameters of the device, primarily by lowering the threshold gate voltage required to create the inversion layer. In fact, if enough holes are trapped at the interface, an inversion layer may form without applying any voltage at all. For p-channel MOSFETs, the process is similar, except the holes migrate toward the metal-gate contact and are trapped at that interface.

Recent experiments have been conducted by the Air Force Weapons Laboratory to characterize the effects of ionizing radiation on MOSFETs. References 3 and 4 describe this work in detail. Large numbers of non-radiation-hardened Intersil 3N161 p-channel and 3N171 n-channel discrete MOSFETs were irradiated with protons, electrons, and Co-60 gamma rays. After exposure to specified levels of radiation (under various bias conditions), the transistor gate threshold voltages were measured "in situ", and the changes in threshold voltage found as a function of radiation angle of incidence (the angle between the proton track and the electric

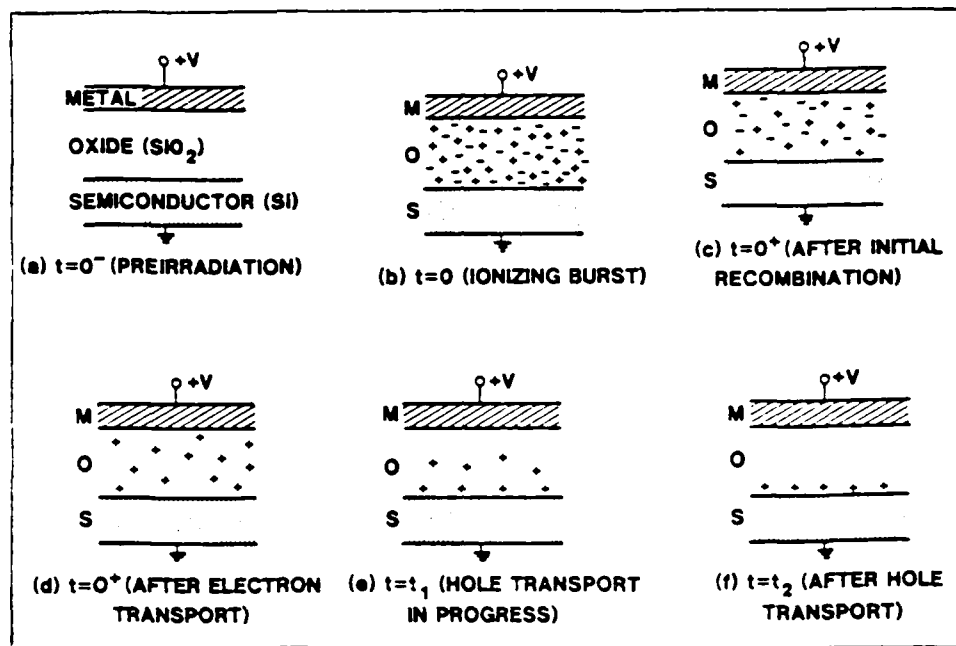


Figure 2. Sequence of Events Associated with Irradiation of MOSFET (Ref 2:67)

field), applied field, particle energy, and total ionizing dose.

Of particular interest were the results of the proton irradiations. In this case, the MOSFETs were irradiated at room temperature with protons of energies from 2-16 MeV. The angle between the proton track and the electric field was varied, and data collected for the cases of 0, 45, and 80 degrees. Figures 3 and 4 show the damage sensitivity (change in threshold voltage per dose) for the p-channel and n-channel MOSFETs, as a function of particle energy and angle of incidence. In general, the damage increases with both particle energy and angle of incidence. This is as expected, as will be explained in the theory section of this paper.

What is not expected, however, is the anomaly where the damage caused by the 45 degree protons is greater than that of the 80 degree protons for particle energies less than 6 MeV. When first observed, the researchers thought that this

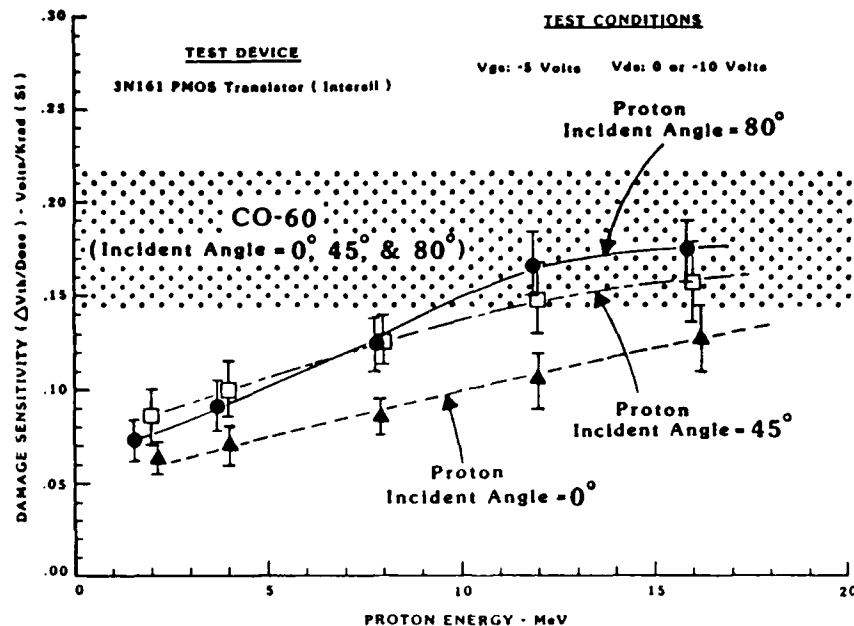


Figure 3. P-channel MOSFET Damage Sensitivity as a Function of Particle Energy and Angle of Incidence (Ref 4:1209)

anomaly was due to the additional material (silicon dioxide passivation and aluminum metallization) the 80 degree protons had to pass through before reaching the gate oxide. If these additional material lengths were greater than the mean proton ranges, then the number of 80 degree protons reaching the gate oxide would be reduced. However, the actual distance traveled by the protons was found to be 6 to 7 times less than the mean ranges of 2-6 MeV protons. This implied that all of the protons reached and passed through the gate oxide, regardless of the angle of incidence.

In a further attempt to understand this anomaly, the data was replotted in a different format, shown in Figures 5, 6, and 7. Figure 5 shows the change in threshold voltage as a function of dose for the various angles of incidence. For this case, the gate bias potential was -5 Volts. Figures 6 and 7 show essentially

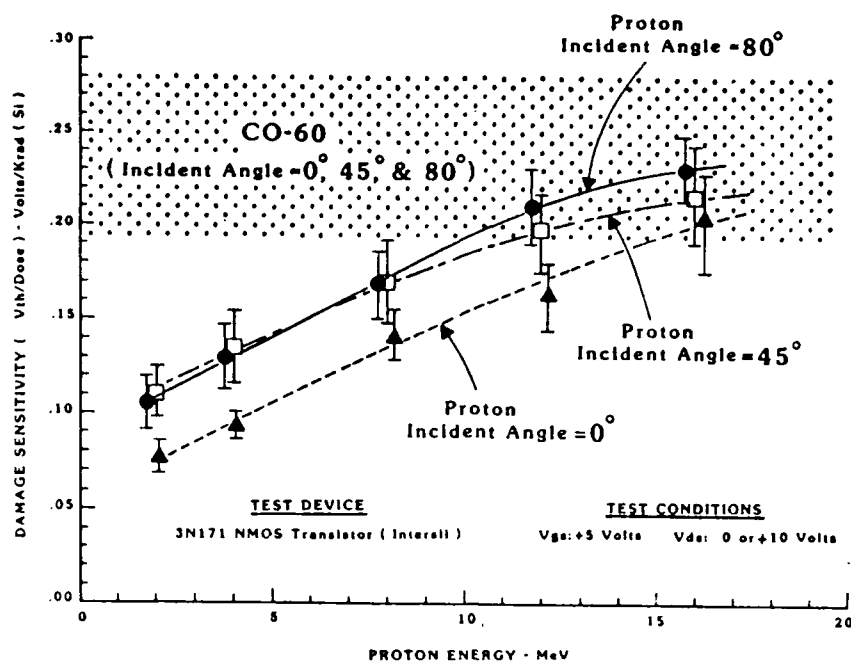


Figure 4. N-channel MOSFET Damage Sensitivity as a Function of Particle Energy and Angle of Incidence (Ref 4:1209)

the same thing, though with different gate bias potentials. On the basis of these graphs, the researchers deduced that a saturation effect was occurring within the test sample, that had the same effect as reducing the internal electric field during irradiation.

To explain this phenomena, the researchers proposed that the buildup of trapped holes at the interface resulted in a counter electric field. The yield fraction of holes escaping initial recombination increases with both the angle of incidence and the magnitude of the electric field. Initially, the higher yield fraction of the 80 degree protons results in a larger charge buildup at the interface. However, this larger buildup offsets the electric field within the oxide, decreasing the fraction of holes escaping recombination. Thus, the threshold voltage change due to 80 degree protons saturates before the 45 degree case.

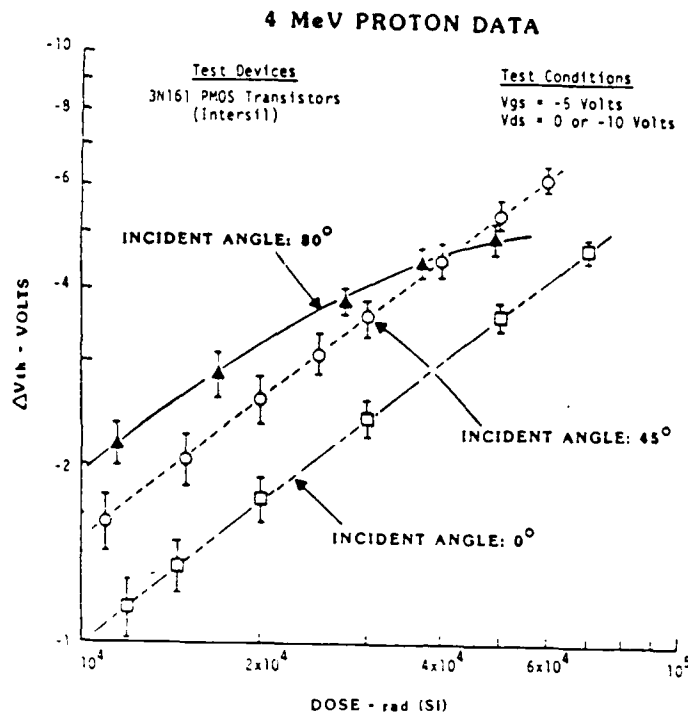


Figure 5. Change in Threshold Voltage as a Function of Dose and Angle of Incidence for Applied Gate Voltage of -5 Volts (Ref 4:1212)

The goal of this thesis project was to give this rough qualitative model a more precise quantitative formulation, and verify that the counterfield effect actually explains the anomaly. The next section describes the stages shown in Figure 2 in more detail. Assumptions used in the model are stated, and mathematical formula presented. The following section presents the major results and analysis, and is, in turn, followed by the conclusion.

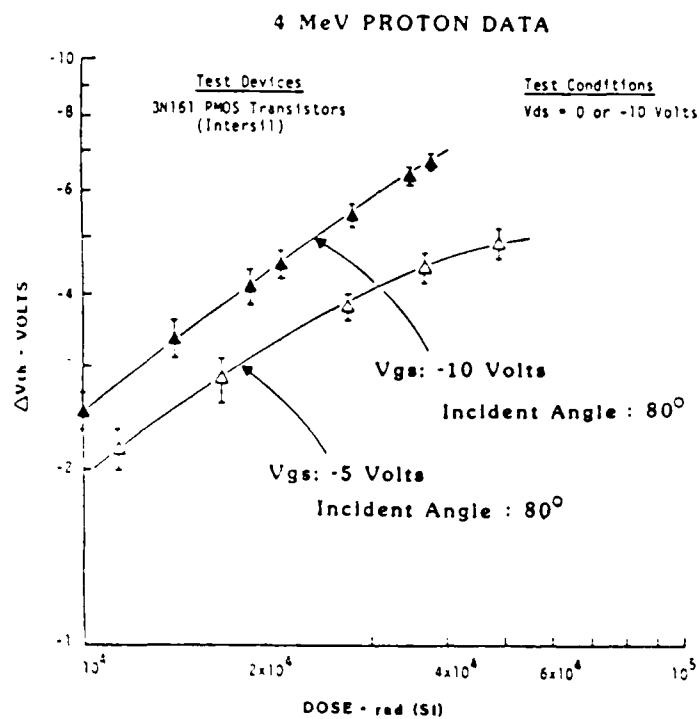


Figure 6. Change in Threshold Voltage as a Function of Dose for 80 Degree Angle of Incidence and Gate Voltages of -5 and -10 Volts (Ref 4:1213)

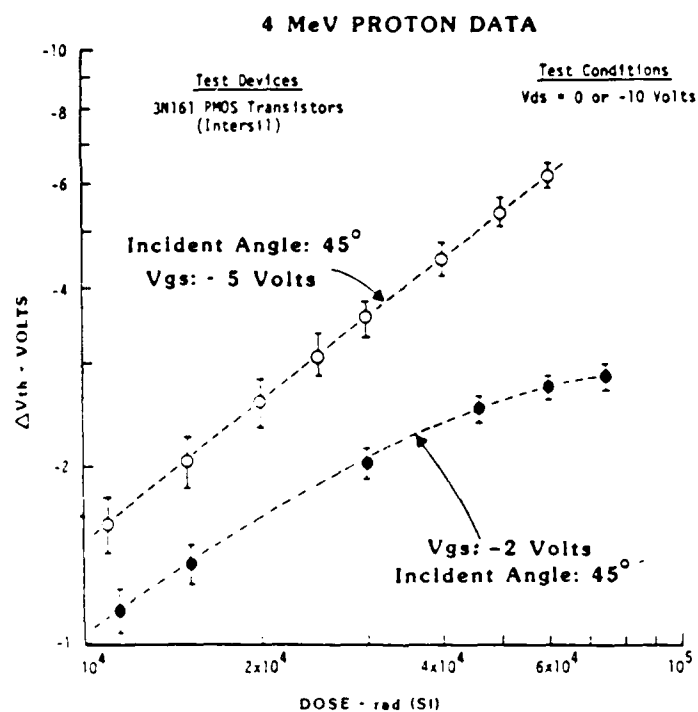


Figure 7. Change in Threshold Voltage as a Function of Dose for 45 Degree Angle of Incidence and Gate Voltages of -2 and -5 Volts (Ref 4:1213)

II. Theory

This section describes the assumptions and mathematical equations that enter into each stage of the model. Considered in turn are columnar phenomena including initial electron-hole formation and recombination, bulk phenomena including electron and hole transport, and interface phenomena including deep-hole trapping, and radiation-induced traps. Following this, an equation relating the change in threshold voltage to the total ionizing dose is developed. Both the dependence of the electric field on trapped charge, and the dependence of yield fraction escaping recombination on electric field are considered in this development.

Columnar Phenomena

As the protons pass through the oxide, they lose energy through ionization and excitation of electrons across the energy bandgap; electron-hole pairs are formed. The amount of energy needed to create an electron-hole pair in silicon dioxide has been estimated to be about 18 eV (Ref 5:1520). Protons, as well as other heavy charged particles, leave a very dense column of electron-hole pairs in their track. However, to determine the initial charge produced by an incremental dose, the electron-hole pairs are assumed to be evenly distributed throughout the bulk of the oxide. This incremental charge is given as

$$\Delta C = K_g \Delta D A f_v \quad (1)$$

where

$$\Delta C = \text{charge (Coulomb)}$$

K_g = generation constant (Coulomb/cm³-rad)
 ΔD = dose (rad-SiO₂)
 A = area of oxide (cm²)
 l = length of oxide (cm)
 f_y = fraction yield

The generation constant, K_g , is found from

$$K_g = \frac{(.01 \text{ J/kg-rad})(1.609 \times 10^{-19} \text{ C/hole})\rho}{(1.609 \times 10^{-19})(1000 \text{ g/kg})W} \quad (2)$$

where

ρ = density (g/cm³)
 W = energy per electron-hole pair formed (eV/hole)

For SiO₂ the density is 2.2 g/cm³ and the energy required to form an electron hole pair is 18 eV. Filling these numbers into Eq (2) gives a generation constant of 1.222×10^{-6} Coulomb/cm³-rad.

Immediately after the electron-hole pairs are produced in the dense column, a certain fraction of them will recombine. The fraction that survive, f_y , is a function of the particle type and energy, the electric field within the oxide, and the incident angle between the particle track and electric field. To find the fraction yield, a numerical procedure developed by Oldham (described in references 6 and 7) is used. A description of this procedure follows.

Figure 8 shows a schematic of the track of a charged particle after passing through the silicon dioxide insulator. Looking down the direction of the track, the initial charge density configuration is assumed to be

$$n_{\pm} = \frac{N_o}{\pi b^2} e^{-r^2/b^2} \quad (3)$$

where

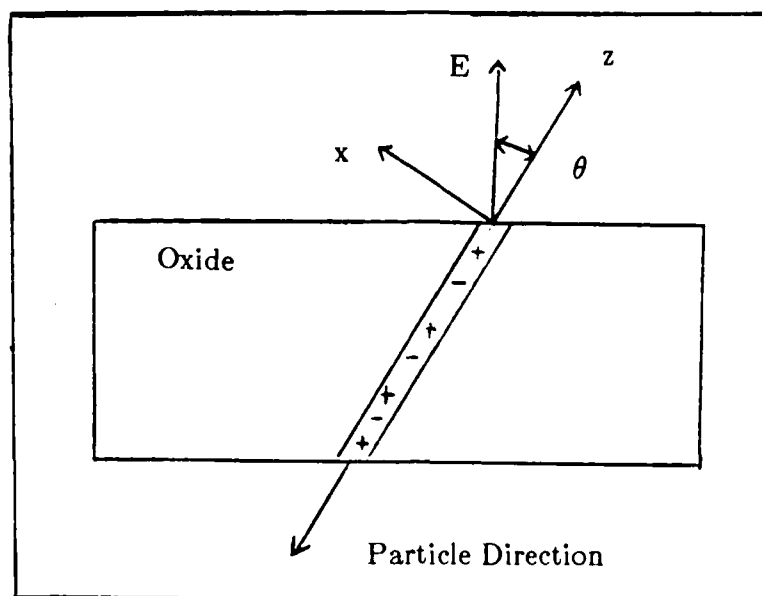


Figure 8. Charged Particle Track Through the Oxide

n_{\pm} = electron-hole density (cm^{-3})

N_0 = initial linear density (cm^{-1})

b = Gaussian radius (cm)

r = Distance center of the track (cm)

The electrons and holes then move according to the equation (Ref 7:2695)

$$\frac{\partial n_{\pm}}{\partial t} = D_{\pm} \nabla^2 n_{\pm} + \mu_{\pm} E_x \frac{\partial n_{\pm}}{\partial x} - \alpha n_+ n_- \quad (4)$$

where

D_{\pm} = Diffusion coefficient (cm^2/s)

μ_{\pm} = mobility ($\text{cm}^2/\text{V-s}$)

E_x = Component of electric field in the x-direction (V/cm)

α = Recombination coefficient (cm^3/s)

The first term on the right hand of Eq (4) represents diffusion, the second term represents drift under the influence of the external field, and the third term represents recombination.

The actual program (found in the Appendix) sets up a grid in the x and y-direction with z in the direction of the proton track, and y perpendicular to the electric field for all proton angles of incidence. The initial electron-hole density is found from Eq (3) for each point in the grid. These densities are then placed into a finite difference form of the right hand side of Eq (4), and $\partial n_{\pm}/\partial t$ found at each point on the grid. The new densities are then found from

$$n_{\pm}(r, t_{\text{new}}) = n_{\pm}(r, t_{\text{old}}) + \frac{\partial n_{\pm}}{\partial t} \Delta t \quad (5)$$

where Δt is the increment in time. These new densities are inserted into the right hand side of Eq (4), and the process repeated until the electron and hole columns separate under the influence of the external field. Integrating $n_{+}(r, t)$ over the area of the grid gives a new linear hole density $N(t)$.

Figure 9 shows the electron-hole columns moving past each other under the influence of an electric field of arbitrary direction. For the case of a particle track perpendicular to the electric field, the fraction yield, f_y , will be given simply by $N(t)/N_0$, where $N(t)$ is the linear density after the columns have separated. The analysis up to this point is only good for the region between the dashed lines in Figure 9, but it can be generalized to three dimensions. If it is assumed that the hole column to the right of the right-hand dashed line remains unchanged, then the fraction yield can be found from

$$f_y = \frac{\int_0^T N(t) dt}{N_0 T} \quad (6)$$

where T is the time required for the right hand of the electron column to cross the left hand of the hole column.

The parameters μ_{\pm} , D_{\pm} , α , N_0 , and b in Eqs (3) and (4) are found in the following way. The room temperature mobilities of silicon dioxide are found quite

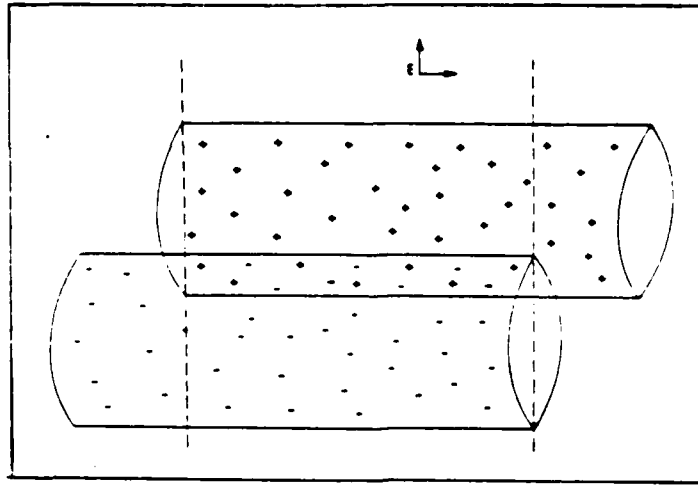


Figure 9. Electron and Hole Columns Moving Under the Influence of Arbitrary Electric Field (Ref 7:2696)

readily from the literature. The values used in this analysis were

$\mu_+ = 2 \times 10^{-5} \text{ cm}^2/\text{V}\text{-sec}$ (Ref 8:2012) and $\mu_- = 20 \text{ cm}^2/\text{V}\text{-sec}$ (Ref 9:1333). The diffusion coefficients, D_{\pm} , are then found from the mobilities by using the Einstein relation (Ref 7:2696)

$$D_{\pm} = \frac{\mu_{\pm} kT}{e} \quad (7)$$

where k is the Boltzmann constant, T is the temperature, and e is the electron charge. The recombination coefficient, α , is found by using an expression derived by Langevin (Ref 7:2696)

$$\alpha = \frac{(\mu_+ + \mu_-)e}{\epsilon \epsilon_0} \quad (8)$$

where ϵ is the dielectric constant of silicon dioxide, and ϵ_0 is the permittivity of free space. The initial linear density, N_0 , depends on particle energy and can be found from stopping power tables (Ref 10:310). The value of the Gaussian radius, b , was taken from Reference 7 where it was used as a variable parameter to fit

this recombination model to experimental data. The value was found to be 3.5 nanometers (Ref 7:2697).

It should be pointed out that this model is only valid for situations where the electron-hole pair separation distance is short enough that the pairs lose their identity. In this case electrons readily recombine with holes from different pairs. This is generally true of the particle tracks left by heavy charged particles, because of their high linear energy transfer. For electrons and gamma-rays, the pair separation distance is large enough that recombination is pretty much restricted to electron-holes of the same pair. The model developed to handle these cases is called the geminate model (Ref 1:27).

In general, the yield fraction f_y depends on three factors. First, it depends on the energy of the particle. This is because the initial linear density, N_0 in Eq (3), generally decreases with increasing particle energy, at least in the ranges of interest here. The lower the initial density, the less probability there is that recombination will occur, thus the yield fraction increases. Second, yield fraction also depends on the strength of the electric field. The stronger the field, the more quickly the electron and hole columns separate, decreasing the time available for recombination. Thus, yield fraction increases with increasing electric field. Third, the yield fraction depends on the angle of incidence. This can be understood by considering the two extremes. When the particle track is perpendicular to the field, the two columns are separated rapidly, which increases yield fraction. When the particle track is parallel to the field, the columns are pulled through each other, enhancing recombination, and reducing the yield fraction. Thus, yield fraction increases with increasing angle of incidence.

This increase in yield fraction with particle energy, electric field and angle of incidence is the cause of the general characteristics of the curves seen in Figures 3 through 7. In these figures, the change in threshold voltage also increases with

particle energy, electric field, and (except for particle energies below 6 MeV) angle of incidence. As will be seen below, the change in threshold voltage is directly proportional to the charge accumulated at the interface of the oxide and thus the yield fraction.

Bulk Phenomena

After escaping initial recombination the remaining electrons are rapidly swept from the oxide by the applied gate field. This process takes a few picoseconds to complete. Two assumptions are made about this stage. First, no electrons are trapped within the oxide. Second, having escaped columnar recombination, the electrons do not recombine further with holes previously trapped in the oxide.

After the electrons are swept from the device, the holes transport toward the interface much more gradually. Assume all the holes move with the same velocity, $v = \mu_p E$. For an oxide of length 280 nanometers and an electric field of 1×10^5 V/cm at room temperature, it takes a hole 1.40×10^{-5} seconds to cross the oxide. This time is short enough to justify ignoring any transient effects caused by transport. To simplify the analysis then, all the holes produced by an incremental dose, ΔD (that escape recombination), are assumed to instantaneously transport to the interface. Bulk trapping within the oxide is ignored.

Interface Phenomena

As the holes pass through the interface region, a certain fraction, f_T , are caught in deep hole traps within about 10 nanometers of the interface. The fraction trapped depends on the temperature and electric field, but is mostly a result of the processing techniques used during manufacture. The interface region has

high local strain and a deficiency of oxygen atoms. This gives rise to a large number of Si-Si bonds instead of the usual Si-O-Si bonds found in silicon dioxide. When a hole passes one of these bonds, it can break the bond and recombine with one of the bonding electrons. This results in a Si atom retaining the remaining electron from the broken bond, and the positive charge residing with the other Si atom (Ref 1:34).

Since the trapping fraction depends primarily on the manufacturing process, it can vary quite radically between different MOSFETs. Generally, f_T can be as little as 1-2 percent for hard oxides, 10-20 percent for good quality commercial oxides, and as much as 50-70 percent in very soft commercial oxides (Ref 1:33).

The spatial dependence of the charge trapped at the interface is also dependent on the relative hardness of the device. Hard oxides have distributions that fall off exponentially as one moves away from the interface into the oxide. On the other hand, the softer oxides have distributions that remain relatively constant (Ref 11:1207).

These trapped holes can persist from a few hours to years. Annealing does take place, in which electrons from the Si semiconductor tunnel into the oxide and recombine with the trapped holes. However, since the time frame for annealing is considerably longer than the experiment, it is ignored in this model.

This model assumes that a certain fraction, f_T , of the holes escaping recombination will be trapped in a constant charge distribution, ρ , extending a distance X from the interface. The incremental charge density due to an incremental dose is then

$$\Delta\rho = \frac{K_g \Delta D f_v f_T}{X} \quad (9)$$

in the region near the interface and 0 elsewhere. X is presumably about 10 nm (Ref 1:33). The trapping fraction is uncertain, but since these devices are reported

as non-radiation hardened (Ref 3:4393), it is probably greater than 10 percent. This quantity is left undetermined in the analysis, but is assumed constant.

Radiation-induced interface traps exist very close to the interface, and within the Si band gap. Their occupancy is determined by the position of the Fermi level at the interface, and can be negative (usually with n-channel devices), positive (usually with p-channel devices), or neutral. In either case, the presence of these trapped charges results in shifts to the threshold voltage. At the present time, the precise mechanisms responsible for the formation of these states are not well understood, and a subject of considerable debate (Ref 1:37). These states are difficult to model. Since the deep hole traps are dominant (especially at the lower dose levels applicable here), interface traps are ignored in this analysis.

Threshold Voltage vs Dose

In this section, an analytical expression relating the change in threshold voltage to the total ionizing dose is found, so that the curves in Figures 5 through 7 can be simulated. This expression will include the dependence yield fraction has on electric field and incident angle.

The change in threshold voltage for arbitrary charge density is given by (Ref 12:199)

$$\Delta V_{th} = \int_0^l \frac{-x\rho(x)}{\epsilon} dx \quad (10)$$

where

- l = the length of the oxide (cm)
- $\rho(x)$ = density of holes (cm^{-3})
- ϵ = permittivity of SiO_2

Assuming the charge density is constant between $l - X$ and l , and zero elsewhere,

the threshold voltage change becomes

$$\Delta V_{th} = \frac{\rho(X^2 - 2Xl)}{2\epsilon} \quad (11)$$

or

$$d\Delta V_{th} = \frac{\Delta\rho(X^2 - 2Xl)}{2\epsilon} \quad (12)$$

where $d\Delta V_{th}$ is the incremental change in threshold voltage resulting from an incremental change in charge density. Substituting the value for $\Delta\rho$ given by Eq (9) into Eq (10) gives

$$d\Delta V_{th} = K_g f_y f_T l \frac{(X - 2l)}{\epsilon} \Delta D \quad (13)$$

In Eq (13), everything is assumed constant except the yield fraction, f_y , which depends on the electric field, which in turn depends on the charge distribution.

We next derive an expression relating the internal electric field to ρ and thus ΔV_{th} . Figure 10 shows a schematic cross section of a MOSFET, with an areal density $Q_{x'}$ located at arbitrary x' within the oxide. This charge induces a charge density Q_o at the gate, and Q_l at the semiconductor. Ignoring any difference in work function between the metal gate and semiconductor, it can be shown that

$$Q_o = -\frac{l - x'}{l} Q_{x'} \quad (14)$$

and

$$Q_l = -\frac{x'}{l} Q_{x'} \quad (15)$$

Using Gauss' Law, the internal electric field due to charge density $Q_{x'}$ becomes

$$E(x) = -\frac{(l - x')}{l\epsilon} Q_{x'} \quad (16)$$

for $0 < x < x'$ and

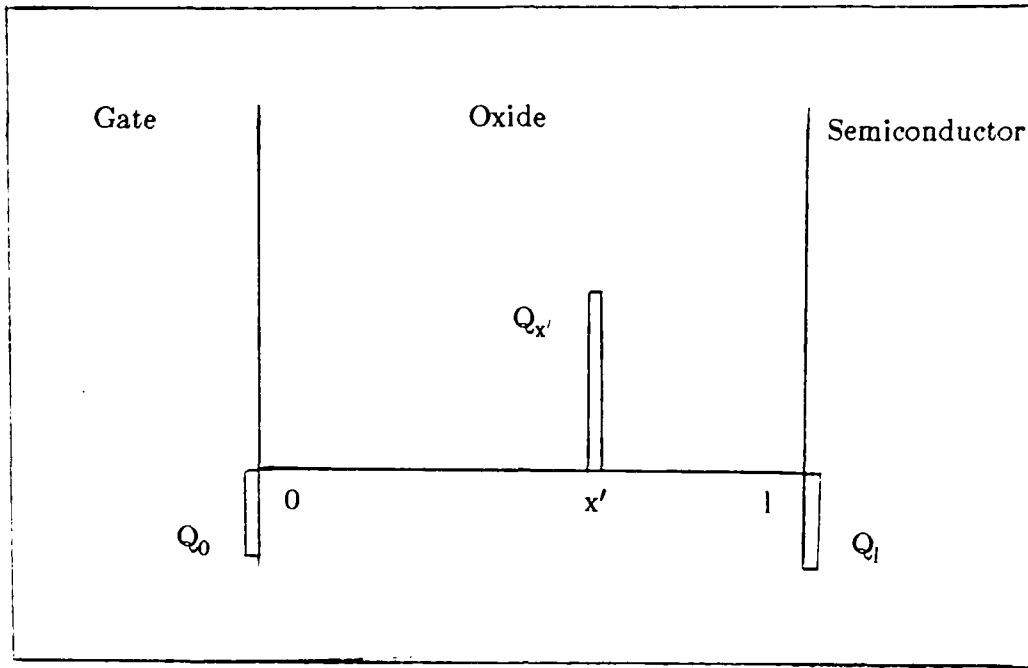


Figure 10. Schematic Cross Section of MOSFET With Arbitrary Areal Charge Density $Q_{x'}$ at x'

$$E(x) = \frac{x'}{l\epsilon} Q_{x'} \quad (17)$$

for $x' < x < l$.

Eqs (16) and (17) can be generalized to an arbitrary charge distribution $\rho(x)$ as shown in Figure 11. Taking into account the field due to the external gate voltage and letting $Q_{x'} = \rho(x')dx'$, the electric field at x becomes

$$E(x) = \int_0^x \frac{x' \rho(x')}{\epsilon} dx' - \int_x^l \frac{(l - x') \rho(x')}{\epsilon} dx' + \frac{V_g}{l} \quad (18)$$

Expanding the second term on the right and rearranging gives

$$E(x) = \int_0^l \frac{x' \rho(x')}{l\epsilon} dx' - \int_x^l \frac{\rho(x')}{\epsilon} dx' + \frac{V_g}{l} \quad (19)$$

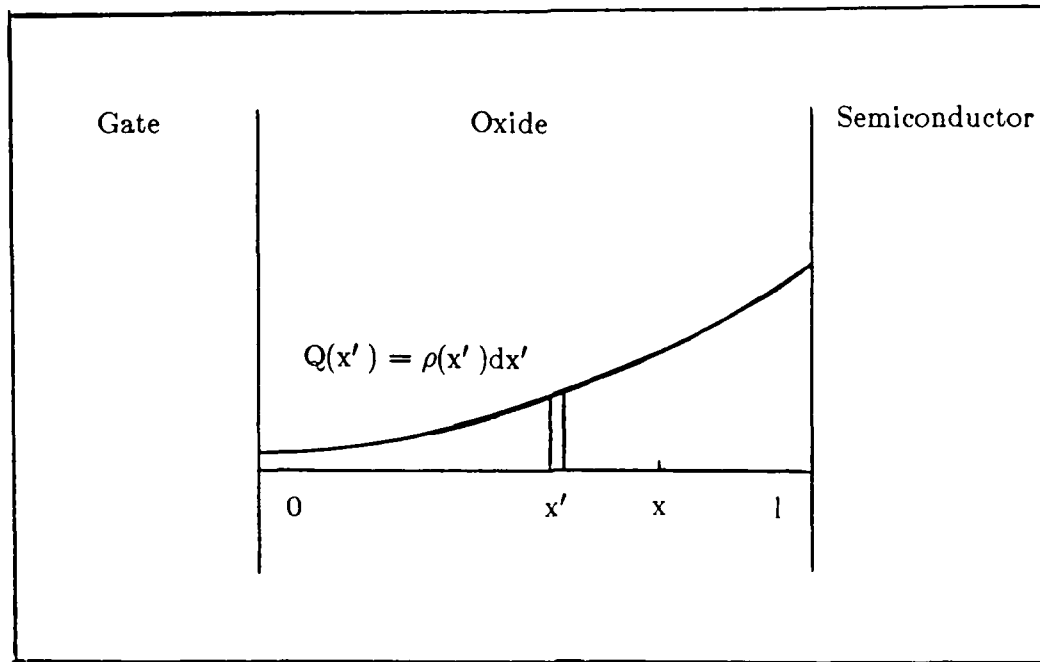


Figure 11. Schematic Cross Section of MOSFET with Arbitrary Charge Density

The first term on the right hand side of Eq (19) is merely $-\Delta V_{th}/l$. Concerning ourselves with the field only at $x < l - X$, the second term becomes $-\rho X/\epsilon$. Finding ρ in terms of ΔV_{th} from Eq (11) and inserting into this second term gives

$$E(x) = \frac{\Delta V_{th}}{l} \left(\frac{X}{2l - X} \right) + \frac{V_g}{l} \quad (20)$$

For simplicity, the yield fraction is assumed linear with electric field and can be given the form

$$f_y(E) = a_\theta E + b_\theta \quad (21)$$

where a_θ and b_θ will depend on the angle of incidence for a proton of given energy. Substituting Eq (20) into Eq (21) will give f_y as a function of change in threshold voltage. Placing $f_y(\Delta V_{th})$ into Eq (14) yields an equation of the form

$$\frac{d\Delta V_{th}}{f_y(\Delta V_{th})} = K_g l f_T \frac{(X - 2l)}{2E} \Delta D \quad (22)$$

Integrating Eq (22), and rearranging, results in an equation relating the threshold voltage change and the dose:

$$\Delta V_{th} = \left(\frac{2l - X}{X} \right) \left(V_g + \frac{b_{\theta} l}{a_{\theta}} \right) \left(\exp \left[\frac{-a_{\theta} X K_g f_T D}{2\epsilon} \right] - 1 \right) \quad (23)$$

III. Results and Analysis

The previous section developed the model used to simulate the effect charged particle radiation has on MOSFET devices. This section describes the results of applying this model to the actual experiment described in the introduction and background section.

Figure 12 shows the yield fraction as a function of particle energy for angles of incidence of 0, 45, and 80 degrees using the columnar recombination model. An electric field of 1.79×10^5 V/cm was used. This field was found by dividing the gate voltage (5 Volts) by the thickness of the oxide (280 nanometers). The fraction yield increases with both particle energy and angle of incidence, and the characteristics of these curves are similar to those shown in Figures 3 and 4 except for the data anomaly.

In finding a functional relationship between the change in threshold voltage and the dose (accounting for oxide field modulation due to hole trapping near at the interface) it was assumed that the fraction yield was a linear function of the electric field within the oxide. Figure 13 shows the fraction yield as a function of electric field for 4 MeV protons with angles of incidence of 45 and 80 degrees. This figure was found by using the columnar recombination model. As can be seen, the fraction yield increases with both electric field and angle of incidence, but the curves are not linear throughout the range of interest. To properly use Eq (23), a linear approximation was taken from 0.1 MV/cm to 0.25 MV/cm (the general range of the oxide electric field during the irradiation). The coefficients in Eq (21) are found to be $a_\theta = 4.11 \times 10^{-7}$ cm/V and $b_\theta = .0539$ for an angle of 45 degrees, and $a_\theta = 4.88 \times 10^{-7}$ cm/V and $b_\theta = .0650$ for an angle of 80 degrees. Using these values in Eq (23) with $X = 10$ nm, $l = 280$ nm, and $V_g = 5$ Volts,

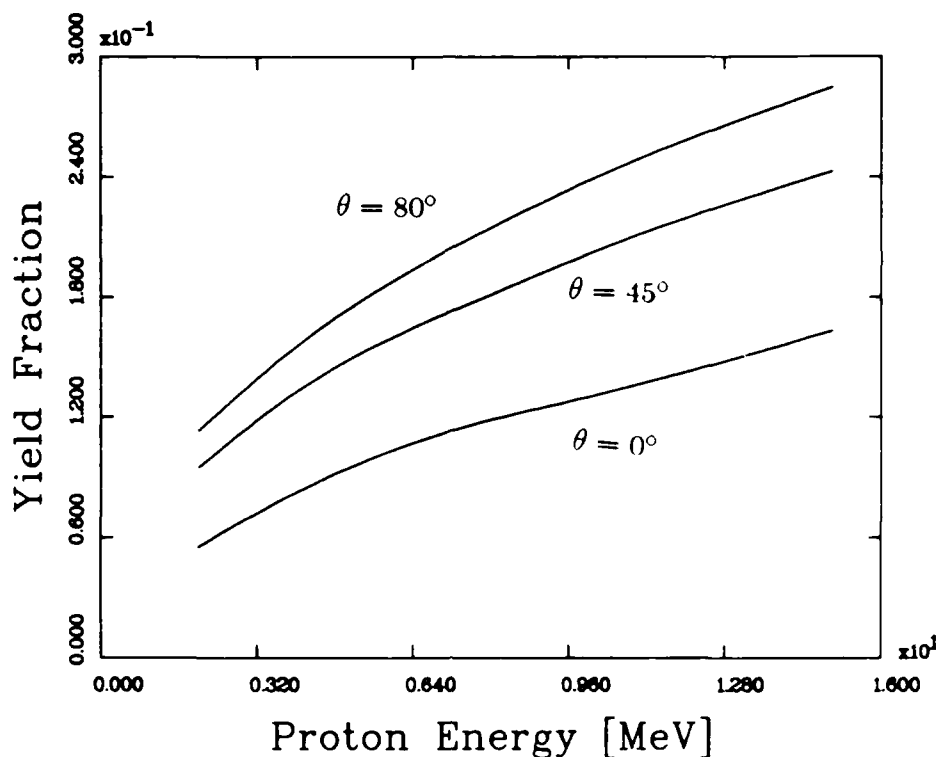


Figure 12. Fraction Yield as a Function of Particle Energy and Angle of Incidence.

ΔV_{th} was found as a function of dose for trapping fractions of .20, and .40. The results are shown in Figure 13. As expected, the threshold voltage rises with dose, angle of incidence, and trapping fraction. However, the sought after saturation effect is missing.

The reason the saturation effect is absent is straightforward. If all of the charge is assumed to accumulate within 10 nm of the interface, the charge giving rise to a threshold voltage change equivalent to the gate voltage will (from Eq (20)) only decrease the internal field to 0.982 of its original value. This is generally true for charges at the interface--they modulate the internal electric field very little, certainly not enough to cause the saturation effect seen in Figures 5

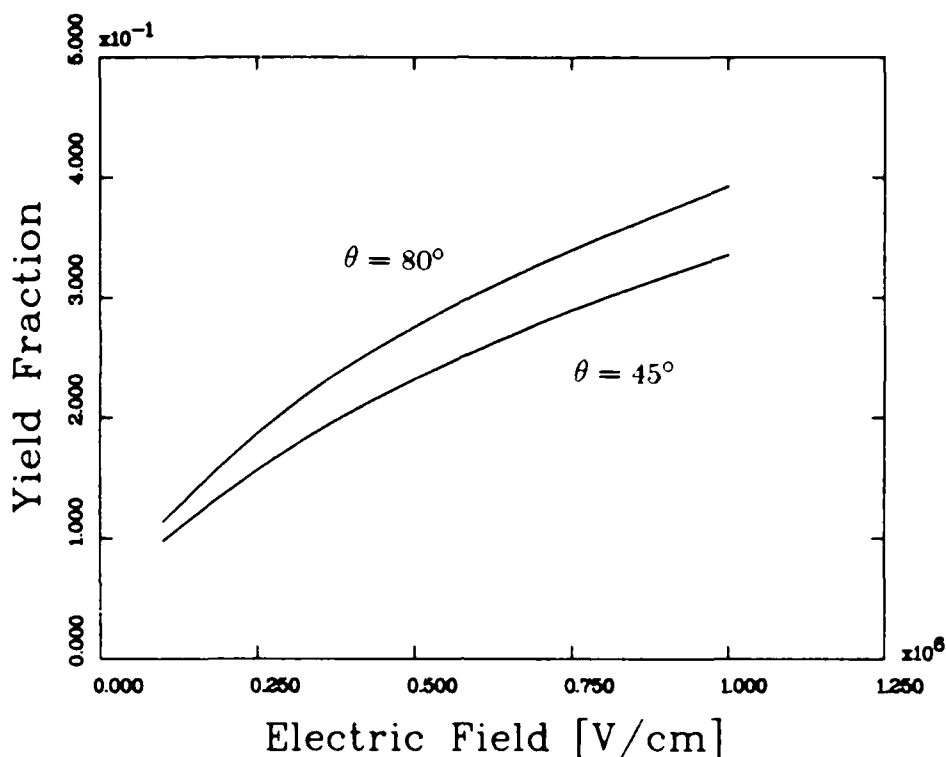


Figure 13. Fraction Yield as a Function of Electric Field and Angle of Incidence

through 7.

This raises the question whether all of the charge is actually trapped near the interface. There is evidence that it is not. Figures 3 and 4 show the damage sensitivity for both n-channel and p-channel MOSFETs. Under applied bias, holes created by radiation accumulate at the gate interface in p-channel MOSFETs, and at the semiconductor interface in n-channel MOSFETs. From Figures 3 and 4, it can be seen that the damage sensitivity is a little bit greater in the n-channel devices, but not much. Our original assumption was that the charge was trapped within 10nm of the interface. Using Eq (10), a given charge, ρ , at the interface of the p-channel device results in a threshold voltage change of $-50\rho/\epsilon$. If this same charge is distributed at the semiconductor interface of the n-channel device, Eq (10) gives a $\Delta V_{th} = -2750\rho/\epsilon$, which is 55 times greater. Of course this assumes

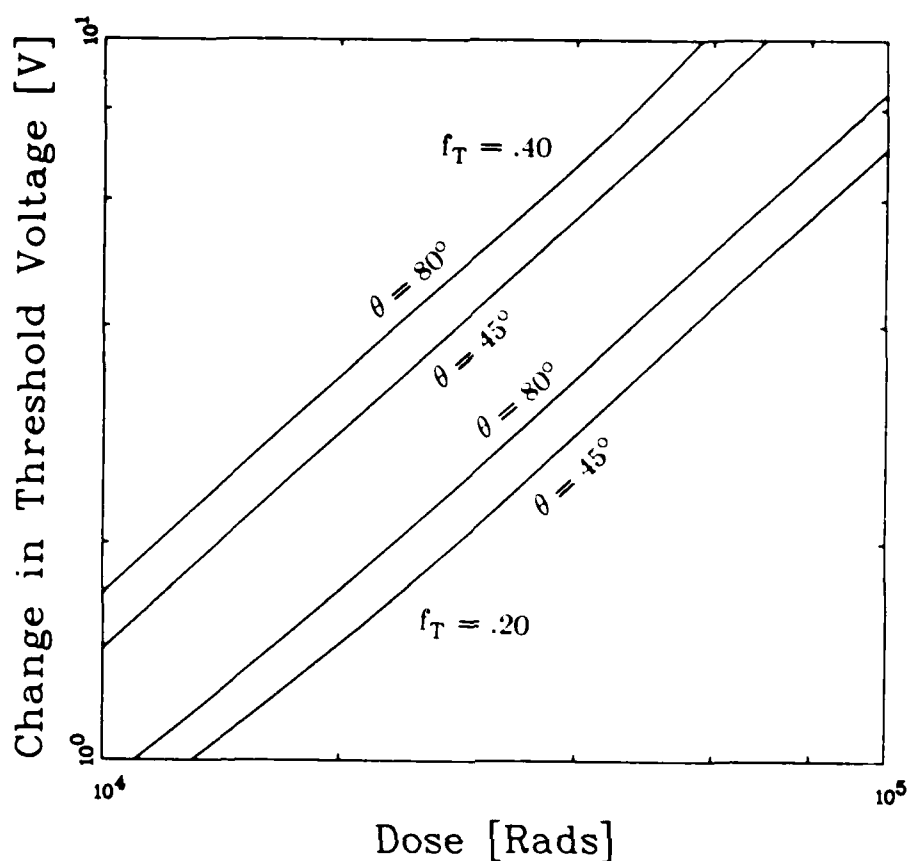


Figure 14. Threshold Voltage Change As a Function of Dose, Angle of Incidence, and Trapping Fraction

the trapping fractions are equal at both interfaces, which is unlikely. However, it seems improbable that the trapping fractions are that different. If a charge ρ is evenly distributed throughout the bulk of the oxide, then the change in threshold voltage is equivalent for both types of MOSFETs.

Thus it appears that there is a significant amount of charge trapped in the bulk of the oxide. The hole transport process is actually very dispersive. Some holes move out of the oxide quickly, while others take a long time to do so. The assumptions made about hole transport trapping are generally true for thin oxides less than 100 nm and high electric fields, greater than 1 MV/cm. For the oxides considered here, the thickness was 280 nm and the field 1.79×10^5 V/cm. With

these parameters, it is likely that a significant proportion of charge is trapped in the bulk of the oxide (Ref 13:3940).

The implication of large bulk trapping can be seen from Figure 15. This figure shows the electric field as a function of distance for a charge density distributed evenly throughout the oxide. The charge density is assumed large enough to give rise to a threshold voltage change equal to the applied gate voltage. From Eqs (11) and (19) the internal electric field is given as

$$E(x) = 2V_g \frac{x}{l^2} \quad (24)$$

so $E(0) = 0$ and $E(l) = 2V_g/l$. The distributed charge causes greater modulation throughout the bulk of the oxide, than that charge accumulated at the surface.

To the left of the midpoint in Figure 15 the electric field falls significantly, causing a reduction in yield fraction. On the other hand, the field rises significantly to the right of the midpoint, which increases the yield fraction. From Figure 13, the yield fraction seems to slope off with decreasing electric field, so the decline in fraction yield in the left hand region may dominate the increase in the right hand side, resulting in an overall reduction in fraction yield. Whether this reduction is great enough to cause the saturation effect remains questionable. It could well be a contributor, but there are other things to consider.

For instance, it was assumed earlier that the electrons, having escaped columnar recombination, were swept from the oxide without further recombination. For low hole densities and high electric fields this assumption is certainly valid. However, the cross section for electron-hole recombination is proportional to $E^{-3/2}$ (Ref 14:3203). The reduced field in Figure 15 could result in significant recombination in the region to the left of midpoint. This could be another source of the saturation effect, especially if the field reaches zero within the oxide. Then the electrons would stop and recombine with a hole (Ref 16:1522-1523).

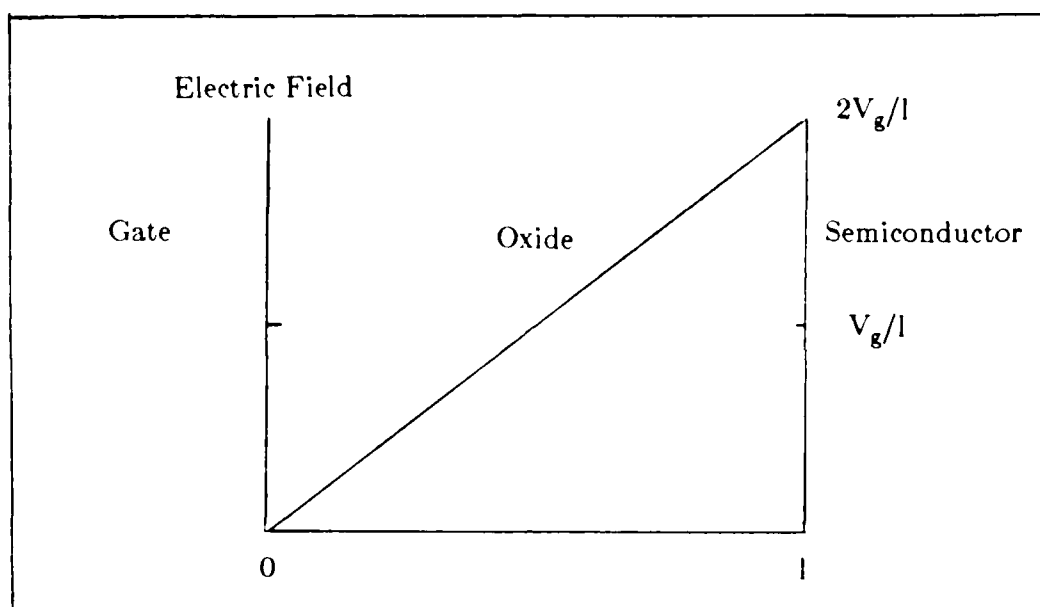


Figure 15. Electric Field Within the Oxide from an Evenly Distributed Charge Density

A third assumption made in this model was that the fraction of holes trapped at the interface was constant. However, it is known that the hole trapping cross section is dependent on the electric field and varies with $E^{-1/2}$ (Ref 15:1192). The increasing field at the interface, as seen in Figure 15 may result in a decline in trapping fraction, that could also be a contributor to the saturation effect.

These three field modulated mechanisms--yield fraction, electron recombination, and hole trapping may all contribute to the saturation effects seen in Figures 5-7. To verify this will require a more refined model that not only takes these mechanisms into account, but also accounts for the wide dispersion inherent in the hole transport. This will be required to characterize the hole buildup in the bulk of the oxide.

IV. Conclusion

In conclusion, this simple model has shown that the electric field reduction due to holes trapped at the interface cannot cause the saturation effect. Charges trapped close to the interface cannot reduce the internal electric field to any great degree--certainly not to the extent required to effect the yield fraction of holes escaping columnar recombination. However, similar p-channel and n-channel damage sensitivities indicate that considerable charge is trapped within the bulk of the oxide. Charge distributed within the oxide bulk modulates the electric field considerably. This modulated electric field could contribute to the saturation effect in three ways-- reduction of the yield fraction throughout the oxide, increase in electron recombination, reduction of hole trapping at the interface.

To verify this, the present model would have to be refined in a number of ways. First, the dispersive nature of hole transport would have to be considered so that reasonable estimates of the trapped hole distribution (both at the interface and within the bulk of the oxide) can be made. Second, Eqs (10) and (19) would have to be modified to numerically find the threshold voltage and electric field for an arbitrary charge density. Third, the nonlinearity between yield fraction and electric field would have to be accounted for, so that overall yield fraction due to a widely varying internal electric field may be found. Fourth, the electron transport and electric field dependent recombination cross section would have to be introduced. Finally, the hole capture cross section dependence on electric field would have to be taken into account. Introducing these refinements into the model should allow determination of the primary cause of the saturation effect and explain the data anomaly.

Appendix: Columnar Recombination Computer Code

This appendix contains the code used to find the yield fraction of electrons and holes escaping initial recombination. The following algorithm is used:

- Step 1. Input the initial linear density, the mobilities, the diffusion coefficients, the recombination coefficient, the electric field, the angle of incidence, the column radius, and the length of the oxide (lines 22-23).
- Step 2. Set up the x and y grid. In this case the maximum values in the x and y directions and the number of grid spaces are read in. The program is set up to take advantage of the symmetry in the y direction (lines 30-45).
- Step 3. Input and initialize time related elements. These include the time increment and the ratio of time increments between each step. This ratio is inserted to help shorten the run times. The time variable is initialized and the maximum time calculated (lines 51-53).
- Step 4. Set up boundary conditions on the grid. In this routine the boundaries are assumed large enough that the electrons and holes separate well before the columns reach the boundary time so the electron and hole densities at xmax, xmin, and ymax are all set to zero (lines 58-73).
- Step 5. Determine the linear density of particle at time equal to zero (lines 108-124).
- Step 6. Determine the yield fraction for each time step (lines 132-216).
- Step 7. Determine new time and time ratio (lines 133-134).
- Step 8. Set new boundary condition along ymin (lines 139-142)
- Step 9. Determine the new density at each point on grid (lines 144-183).
- Step 10. Find the diffusion term in Eq (2) (lines 151-160).
- Step 11. Find the drift term in Eq (2) (lines 164-170).
- Step 12. Find the recombination term in Eq (2) (line 174).
- Step 13. Find the time rate of change of the holes electrons (lines 179-180).
- Step 14. Find the new charge density at the new time (lines 188-196).

- Step 15. Find the number of charge carriers per unit length and thus the new yield (lines 200-212).
- Step 16. Print out the time, electron and hole density, and the yield (line 213).

Appendix of variables.

alpha - recombination coefficient in cm^3/sec

b - Gaussian radius in nanometers

bcm - Gaussian radius in centimeters

check - variable used to determine whether the point is outside the column or not

delx - the length of each element in the grid in the x- direction in nanometers

dely - the length of each element in the grid in the y- direction in nanometers

delt - the time increment in seconds

derele(i,j) - time rate of change of electron charge density in $/\text{cm}^3 \cdot \text{s}$

derhol(i,j) - time rate of change of hole charge density in $/\text{cm}^3 \cdot \text{s}$

diffn - diffusion term in the electron density rate of change equation

diffp - diffusion term in the hole density rate of change equation

dndx - first derivative with respect to x of electron density

dpdx - first derivative with respect to x of hole den density

dplus - diffusion coefficient of holes in cm^2/s

driftn - drift term in the electron density rate of change equation

driftp - drift term in the hole density rate of change equation

dneg - the diffusion coefficient of the electrons in cm^2/s

d2ndx2 - second derivative with respect to x of the electron density

d2ndy2 - second derivative with respect to y of the electron density

d2pdx2 - second derivative with respect to x of the electron density

d2pdy2 - second derivative with respect to y of the hole density

e - the electric field applied across the oxide in Volts/cm
 $el_{den}(i,j)$ - the electron charge density in charges /cm³
 el_{denx} - the density of electrons along the x axis
 el_{deny} - the density of electrons along the y axis
 el_{enum} - the number of electrons along the y axis in charge/cm
 el_{enum1} - the number of electrons above the y axis in charge/cm
 el_{enumo} - the total number of electrons equal to $el_{enum} + el_{enum1} * 2$
 h_x - the length of each element in cm in the x direction
 h_y - the length of each element in cm in the y direction
 $hol_{den}(i,j)$ - the hole charge density in charges /cm³
 hol_{denx} - the hole density along the x axis in charges/cm³
 hol_{deny} - the hole density along the y axis in charges/cm³
 hol_{num} - the number of holes along the y axis in charges/cm
 hol_{num1} - number of holes above the y axis in charges/cm
 hol_{numo} - total number of holes equal to $hol_{num} + hol_{num1} * 2$
 $length$ - length of oxide in cm
 m - number of elements between upper and lower boundaries in the grid in x direction
 mid_x - midpoint of the grid in the x direction
 mid_y - midpoint of the grid in the y direction
 μ_{neg} - mobility of electrons in cm²/V*sec
 μ_{plus} - mobility of holes in cm²/V*sec
 n - number of elements between the upper and lower boundaries of the grid in the y direction
 no - initial line density in charges/cm
 $recom$ - recombination term in the density rate of change equation
 θ_{ad} - angle of incidence between the particle track and the electric field in degrees
 θ_{ar} - angle of incidence in radians

time - time for current step

tmax - maximum time for program to run

tration - ratio of delt from one iteration to that of the previous one

x(i) - values of x for each grid point i in nano- meters

xmax - maximum value of x in nanometers

xmin - minimum value of x in nanometers

y(i) - values of y for each grid point i in nano- meters

yield - fraction yield for columnar recombination

ymax - maximum value of y in nanometers

ymin - minimum value of y in nanometers

```

0001 c This code is designed to find the concentration of holes and elec-
0002 c trons(in charges/cm**3) and the yield fraction of holes escaping
0003 c recombination due to interaction of charged particles (alphas and
0004 c protons) with silicon dioxide.
0005
0006 implicit none
0007 real pi,no,muneg,muplus,dneg,dplus,alpha,e,thetad,thetar
0008 real b,bcm,xmax,xmin,ymax,ymin,dex,dely,x(201),y(102)
0009 real delt,eleden(201,102),holden(201,102),check,yield
0010 real derele(201,102),derhol(201,102),hx,hy,tmax,time,length
0011 real elenum,holnum
0012 real elenumo,holnumo,eledenx(201,100),holdenx(201,100)
0013 real eledeny(101,100),holdeny(101,100),elenum1,holnum1,d2ndx2
0014 real d2ndy2,diffr,dndx,driftr,recom,tratio
0015 real d2pdx2,d2pdy2,diffr,driftp,dpdx
0016 integer n,m,midx,midy,i,j
0017 open(unit=1,file='rec.dat',status='old',READONLY)
0018
0019
0020 c This section initializes a number of the constants.
0021
0022 read(1,*)no,muneg,muplus,dneg,dplus,alpha
0023 read(1,*)e,thetad,b,length
0024 pi=3.1416
0025 thetar=thetad*pi/180
0026
0027
0028 c This section sets up the x and y grid.
0029
0030 read(1,*)xmax,xmin,ymax,ymin,m,n
0031 bcm=b*1E-07
0032 midx=m/2+1
0033 midy=2
0034 dex=(xmax-xmin)/m
0035 dely=(ymax-ymin)/n
0036 hx=dex*1E-07
0037 hy=dely*1E-07
0038 x(1)=xmin
0039 y(1)=ymin
0040 do 10 i=2,m+1
0041     x(i)=x(i-1)+dex
0042 10 continue
0043 do 20 j=2,n+1
0044     y(j)=y(j-1)+dely
0045 20 continue
0046
0047
0048 c This section inputs the time related elements such as the time
0049 c increment, and the maximum time considered.
0050
0051 read(1,*)delt,tratio
0052 tmax=(length/cos(thetar))/(muneg*cos(thetar)*e)
0053 time=0.0
0054

```

```

0055
0056 c   This section inputs the boundary conditions for the charge density
0057 c   at xmin and xmax.
0058
0059     do 30 j=2,n+1
0060         eleden(1,j)=0.0
0061         eleden(n+1,j)=0.0
0062         holden(1,j)=0.0
0063         holden(n+1,j)=0.0
0064     30 continue
0065
0066
0067 c   This section inputs the boundary conditions for the charge density
0068 c   at ymax.
0069
0070     do 40 i=2,m
0071         eleden(i,n+1)=0.0
0072         holden(1,n+1)=0.0
0073     40 continue
0074
0075
0076 c   This section initializes the charge densities at time equal zero.
0077
0078     do 50 i=2,m
0079         do 60 j=2,n
0080             check=-(x(i)**2+y(j)**2)/b**2
0081             if(check.lt.-100.00)then
0082                 eleden(i,j)=0.0
0083                 holden(i,j)=0.0
0084             else
0085                 eleden(i,j)=(no/(pi*bcm**2))*exp(-(x(i)**2+y(j)**2)/b**2)
0086                 holden(i,j)=eleden(i,j)
0087             endif
0088         60 continue
0089     50 continue
0090
0091
0092 c   This section finds the charge density along the x and y axis at
0093 c   time equal to zero.
0094
0095     do 70 i=1,m+1
0096         eledenx(i,1)=eleden(i,midy)
0097         holdenx(i,1)=holden(i,midy)
0098     70 continue
0099     do 80 j=1,n+1
0100         eledeny(j,1)=eleden(midx,j)
0101         holdeny(j,1)=holden(midx,j)
0102     80 continue
0103
0104
0105 c   This section determines the total number of charge carriers(per
0106 c   unit length) at time equal to zero.
0107
0108     elenum=0.0

```

```

0109      holnum=0.0
0110      elenum1=0.0
0111      holnum1=0.0
0112      do 90 i=2,m
0113          do 100 j=3,n
0114              elenum1=elenum1+eleden(i,j)*(hx*hy)
0115              holnum1=holnum1+holden(i,j)*(hx*hy)
0116      100  continue
0117      90  continue
0118      do 110 i=2,m
0119          elenum=elenum+eleden(i,2)*hx*hy
0120          holnum=holnum+holden(i,2)*hx*hy
0121      110  continue
0122      elenumo=elenum+elenum1*2
0123      holnumo=holnum+holnum1*2
0124      yield=holnumo*delt
0125      print*,time,elenumo,holnumo,yield
0126      print*, 'max time=',tmax
0127
0128
0129      c      This section determines the time derivative of the charge density
0130      c      the new charge density and the total charge as a function of time.
0131
0132      120  if(time.gt.tmax)go to 130
0133          time=time+delt
0134          delt=delt*tratio
0135          elenum=0.0
0136          holnum=0.0
0137          elenum1=0.0
0138          holnum1=0.0
0139          do 140 i=1,m+1
0140              eleden(i,1)=eleden(i,3)
0141              holden(i,1)=holden(i,3)
0142      140  continue
0143
0144          do 150 i=2,m
0145              do 160 j=2,n
0146
0147
0148      c      This section finds the diffusion term for the electrons from finite
0149      c      difference form.
0150
0151          d2ndx2=(eleden(i+1,j)-2*eleden(i,j)+eleden(i-1,j))/hx**2
0152          d2ndy2=(eleden(i,j+1)-2*eleden(i,j)+eleden(i,j-1))/hy**2
0153          diffn=dneg*(d2ndx2+d2ndy2)
0154
0155      c      This section finds the diffusion term for the holes from finite
0156      c      difference form.
0157
0158          d2pdx2=(holden(i+1,j)-2*holden(i,j)+holden(i-1,j))/hx**2
0159          d2pdy2=(holden(i,j+1)-2*holden(i,j)+holden(i,j-1))/hy**2
0160          diffp=dplus*(d2pdx2+d2pdy2)
0161
0162      c      This section finds the drift term for the electr

```

```

0163
0164      dndx=(eleden(i+1,j)-eleden(i-1,j))/(hx*2)
0165      driftn=muneg*e*sin(thetar)*dndx
0166
0167 c      This section finds the drift term for the holes.
0168
0169      dpdx=(holden(i+1,j)-holden(i-1,j))/(hx*2)
0170      driftp=muplus*e*sin(thetar)*dpdx
0171
0172 c      This section finds the recombination term for both holes and electrons.
0173
0174      recom=-alpha*eleden(i,j)*holden(i,j)
0175
0176 c      This section then finds the time rate of change of the electron and
0177 c      hole density for each x and y.
0178
0179      derele(i,j)=diffn+driftn+recom
0180      derhol(i,j)=diffp+driftp+recom
0181
0182      160      continue
0183      150      continue
0184
0185 c      This section finds the new charge density at each point for
0186 c      new time.
0187
0188      do 170 i=2,m
0189      do 180 j=2,n
0190      eleden(i,j)=eleden(i,j)+derele(i,j)*delt
0191      holden(i,j)=holden(i,j)+derhol(i,j)*delt
0192      if(eleden(i,j).lt.0.0)then
0193      eleden(i,j)=0.0
0194      endif
0195      180      continue
0196      170      continue
0197
0198 c      This section finds the number of charge carriers(per unit length).
0199
0200      do 190 i=2,m
0201      do 200 j=3,n
0202      elenum1=elenum1+eleden(i,j)*(hx*hy)
0203      holnum1=holnum1+holden(i,j)*(hx*hy)
0204      200      continue
0205      190      continue
0206      do 210 i=2,m
0207      elenum=elenum+eleden(i,2)*hx*hy
0208      holnum=holnum+holden(i,2)*hx*hy
0209      210      continue
0210      elenum=elenum1*2+elenum
0211      holnum=holnum1*2+holnum
0212      yield=yield+holnum*delt
0213      print*,time,elenum,holnum,yield
0214
0215      go to 120
0216      130      continue

```

0217
0218
0219
0220

stop
end

Bibliography

1. McLean, F. Barry. *Interactions of Hazardous Environments With Electronic Devices*. Tutorial Short Course, IEEE 1987 Nuclear and Space Radiation Effects Conference. Snowmass Colorado, July 27, 1987.
2. Gover, James E. and Joseph R. Srour. *Basic Radiation Effects in Nuclear Power Electronics Technology*. Sandia Report SAND85-0776, April, 1986.
3. Tallon, Roger W. et al. "A Comparison of Ionizing Radiation Damage In MOSFETs From Cobalt-60 Gamma-rays, 0.5 to 22 MeV Protons and 1 to 7 MeV Electrons", *IEEE Transactions on Nuclear Science*, 32: 4393-4397 (December 1985)
4. Tallon, Roger W. et al. "Radiation Damage In MOS Transistors As A Function of the Angle Of Incidence Between an Applied Field And Various Incident Radiations (Protons, Electrons, and Co-60 Gamma-Rays)", *IEEE Transactions on Nuclear Science*, 34: 1208-1213 (December 1987).
5. Boesch, H. E. and J. M. McGarrity. "Charge Yield and Dose Effects In MOS Capacitors at 80 K", *IEEE Transactions on Nuclear Science*, 23: 1520-1525 (December 1976).
6. Oldham, Timothy R. *Charge Generation and Recombination in Silicon Dioxide from Heavy Charged Particles*, Harry Diamond Laboratories, April 1982 (AD-114713).
7. Oldham, Timothy R. "Recombination Along the Tracks of Heavy Charged Particles in Silicon Dioxide Film", *Journal Applied Physics*, 57: 2695-2702 (April 1985).
8. Hughes, R. C. "Time-resolved Hole Transport in a-SiO₂," *Physics Review B*, 15: 2012-2020 (February 1977).
9. Hughes, R. C. "Charge Carrier Transport Phenomena in Amorphous Silicon Dioxide," *Physics Review Letters*, 30: 1333-1336 (June 1973).
10. Janni, J. F. "Proton Range-Energy Tables 1 keV-10 GeV," *Atomic Data and Nuclear Data Tables*, 27:147-339 (March/May 1982).
11. Oldham T. R. "Spatial Dependence of Trapped Holes Determined From Tunneling Analysis and Measured Annealing," *IEEE Transactions on Nuclear Science*, 33: 1203-1209 (December 1982).
12. Sze S. M., *Semiconductor Devices Physics and Technology* New York: John Wiley and Sons, 1985.

13. Boesch H. E. and F. B. McLean. "Hole Transport and Trapping in Field Oxides," *IEEE Transactions on Nuclear Science*, 32: 3940-3945 (December 1985).
14. Ning, T. H. "High-Field Capture of Electrons by Coulomb Attractive Centers in Silicon Dioxide", *Journal of Applied Physics*, 47: 3203-3208 (July 1976).
15. Boesch, H. E. et al. "Saturation of Threshold Voltage Shift In MOSFETs At High Total Dose", *IEEE Transactions on Nuclear Science*, 33: 1191-1197 (December 1986).
16. Boesch, H. E. and J. M. McGarrity. "Charge Yield and Dose Effects in MOS Capacitors at 80 K", *IEEE Transactions on Nuclear Science*, 23: 1520-1525 (December 1976).

Vita

Captain Kevin M. Kattner was born on 1 May 1958 in Chicago, Illinois. He graduated from high school in Council Bluffs, Iowa, in 1976. He enlisted in the USAF in 1977, and served three years as an aircraft armaments maintenance specialist at Ellsworth AFB, South Dakota. Thereafter he returned to school at Iowa State University under the Airman Education Commissioning Program, where he received the degree of Bachelor of Science in Nuclear Engineering in May of 1983. After graduation, he received a commission in the USAF through Officer Training School. He then served as a foreign technology analyst at the Foreign Technology Division, Wright Patterson AFB, Ohio, until entering the School of Engineering, Air Force Institute of Technology, in August 1986.

Permanent address: 378 Cottonwood Court

Fairborn, Ohio 45432

REPORT DOCUMENTATION PAGE

Form Approved
OMB No. 0704-0188

1a. REPORT SECURITY CLASSIFICATION UNCLASSIFIED		1b. RESTRICTIVE MARKINGS	
2a. SECURITY CLASSIFICATION AUTHORITY		3. DISTRIBUTION / AVAILABILITY OF REPORT Approved for public release; distribution unlimited.	
2b. DECLASSIFICATION / DOWNGRADING SCHEDULE		5. MONITORING ORGANIZATION REPORT NUMBER(S)	
4. PERFORMING ORGANIZATION REPORT NUMBER(S) AFIT/GEP/GNE/88M-4		7a. NAME OF MONITORING ORGANIZATION	
6a. NAME OF PERFORMING ORGANIZATION School of Engineering	6b. OFFICE SYMBOL (if applicable) AFIT/ENP	7b. ADDRESS (City, State, and ZIP Code)	
6c. ADDRESS (City, State, and ZIP Code) Air Force Institute of Technology Wright Patterson AFB OH 45433-6583		9. PROCUREMENT INSTRUMENT IDENTIFICATION NUMBER	
8a. NAME OF FUNDING / SPONSORING ORGANIZATION	8b. OFFICE SYMBOL (if applicable)	10. SOURCE OF FUNDING NUMBERS	
8c. ADDRESS (City, State, and ZIP Code)		PROGRAM ELEMENT NO	PROJECT NO
		TASK NO	WORK UNIT ACCESSION NO
11. TITLE (Include Security Classification) MODELING THE EFFECTS OF HEAVY CHARGED PARTICLES ON METAL-OXIDE-SEMICONDUCTOR FIELD EFFECT TRANSISTORS			
12. PERSONAL AUTHOR(S) Kevin M. Kattner, B.S., Capt, USAF			
13a. TYPE OF REPORT MS Thesis	13b. TIME COVERED FROM _____ TO _____	14. DATE OF REPORT (Year, Month, Day) 1988 March	15. PAGE COUNT 46
16. SUPPLEMENTARY NOTATION			
17. COSATI CODES		18. SUBJECT TERMS (Continue on reverse if necessary and identify by block number)	
FIELD	GROUP	SUB-GROUP	
09	07		
		Radiation Damage, Metal Oxide Semiconductors, Charged particles, Silicon Dioxide	
19. ABSTRACT (Continue on reverse if necessary and identify by block number)			
Thesis Chairman: Michael Sabochick, Captain, USAF Assistant Professor of Nuclear Engineering			
20. DISTRIBUTION / AVAILABILITY OF ABSTRACT <input checked="" type="checkbox"/> UNCLASSIFIED/UNLIMITED <input type="checkbox"/> SAME AS RPT <input type="checkbox"/> DTIC USERS		21. ABSTRACT SECURITY CLASSIFICATION UNCLASSIFIED	
22a. NAME OF RESPONSIBLE INDIVIDUAL Michael Sabochick, Captain, USAF		22b. TELEPHONE (Include Area Code) (513) 255-1012	22c. OFFICE SYMBOL AFIT/ENP

Michael Sabochick 21 Mar 88

UNCLASSIFIED

19. Abstract

A simple model to characterize the effects of heavy charged particles on metal-oxide semiconductor field-effect transistors (MOSFET) is presented. The model is applied to experimental results provided by the Air Force Weapons Laboratory, and an attempt made to simulate saturation phenomena observed in the threshold voltage change. The model assumes all trapped holes are within a few nanometers of the oxide-semiconductor interface, and takes into account the resultant counter electric field, and its effect on the fraction escaping recombination. An equation relating threshold voltage change as a function of dose is derived and used, but does not duplicate the saturation effect. This is because the charge trapped near the interface reduces the internal oxide electric field very little. However, similarities in p-channel and n-channel MOSFET damage sensitivities indicate considerable bulk charge trapping. This would modulate the internal electric field considerably. To determine whether this accounts for saturation will necessitate refinement of the model, taking hole transport and bulk trapping into account.

UNCLASSIFIED

END
DATE
FILMED

4-88
DTIC